

## Universal properties of hard-core bosons confined on one-dimensional lattices

Marcos Rigol and Alejandro Muramatsu

*Institut für Theoretische Physik III, Universität Stuttgart, Pfaffenwaldring 57, D-70550 Stuttgart, Germany*

(Received 12 January 2004; published 27 September 2004)

Based on an exact treatment of hard-core bosons confined on one-dimensional lattices, we obtain the large distance behavior of the one-particle density matrix, and show how it determines the occupation of the lowest natural orbital in the thermodynamic limit. We also study the occupation  $\lambda_\eta$  of the natural orbitals for large- $\eta$  at low densities. Both quantities show universal behavior independently of the confining potential. Finite-size corrections and the momentum distribution function for finite systems are also analyzed.

DOI: 10.1103/PhysRevA.70.031603

PACS number(s): 03.75.Hh, 05.30.Jp

Trapped atomic gases at very low temperatures became in the past years a center of attention in atomic and condensed matter physics. Particularly interesting is the case where the dynamics of the system is restricted to one-dimension (1D) due to a strong transversal confinement. It has been shown recently [1] that in regimes of large positive scattering length, low densities, and low temperatures, a quasi-1D gas of bosons behaves as a gas of impenetrable particles, i.e., as hard-core bosons (HCB). Ultracold Bose gases in 1D have been realized experimentally [2], so that it is expected that soon it will be possible to make the 1D HCB gas a physical reality.

The 1D gas of HCB was first introduced theoretically by Girardeau [3], who also established its exact mapping to a gas of noninteracting spinless fermions. Since then, it remained a subject of recurring attention, and a number of exact results were obtained for the momentum distribution function (MDF)  $n(k)$  and the one-particle density matrix (OPDM)  $\rho(x)$  in the homogeneous [4,5] and the periodic [6] case. It was shown that  $n(k) \sim |k|^{-1/2}$  for  $k \rightarrow 0$ , and that such a singularity arises due to the asymptotic behavior  $\rho(x) \sim |x|^{-1/2}$  for large  $x$  [5,6]. Similar results can be obtained using the hydrodynamic approximation (bosonization) [7].

Recently, the attention has been concentrated on the ground state properties of the 1D gas of HCB confined by a harmonic potential [8], as a model for the experiments. It was found that the occupation of the lowest natural orbital (NO) of the trapped system scales as  $\sqrt{N_b}$ , where  $N_b$  is the total number of particles, as in the homogeneous case (the NO are defined as the eigenstates of the OPDM [9]). The results in 1D are in contrast with higher dimensional systems, where a Bose-Einstein condensate (BEC) was proved to exist [10], and complement that proof by showing that in 1D only a quasicondensate is possible. The introduction of an optical lattice opens new possibilities to engineer strongly interacting states in the trapped gases [11]. Unfortunately, much less is known in the lattice case with confinement.

We present here an exact study of trapped HCB on a lattice. By means of the Jordan-Wigner transformation [12] we calculate exactly the Green's function for large systems (up to  $10^4$  lattice sites). We find that the OPDM  $\rho_{ij} \sim x^{-1/2}$  ( $x = |x_i - x_j|$ ) for large  $x$ , irrespective of the confining potential chosen, even when portions of the system reach occupation  $n_i = 1$ , such that coherence is lost there. The

power law above is shown to determine the scaling of the occupation of the lowest NO in the thermodynamic limit (TL). In addition we find a power-law decay of the NO occupations ( $\lambda_\eta$ ) for large- $\eta$  at low densities, and show that its exponent is also universal.

We consider HCB on a lattice with a confining potential with the following Hamiltonian

$$H_{HCB} = -t \sum_i (b_i^\dagger b_{i+1} + \text{H.c.}) + V_\alpha \sum_i x_i^\alpha n_i, \quad (1)$$

with the addition of the on-site constraints  $b_i^{\dagger 2} = b_i^2 = 0$ ,  $\{b_i, b_i^\dagger\} = 1$ . The creation and annihilation operators for the HCB are given by  $b_i^\dagger$  and  $b_i$  respectively,  $n_i = b_i^\dagger b_i$  is the particle number operator,  $t$  is the hopping parameter and the last term in Eq. (1) describes an arbitrary confining potential, with power  $\alpha$  and strength  $V_\alpha$ .

The Jordan-Wigner transformation,

$$b_i^\dagger = f_i^\dagger \prod_{\beta=1}^{i-1} e^{-i\pi f_\beta^\dagger f_\beta}, \quad b_i = \prod_{\beta=1}^{i-1} e^{i\pi f_\beta^\dagger f_\beta} f_i, \quad (2)$$

maps the HCB Hamiltonian into the one of noninteracting fermions  $H_F = -t \sum_i (f_i^\dagger f_{i+1} + \text{H.c.}) + V_\alpha \sum_i x_i^\alpha n_i^f$ , with  $f_i^\dagger$  and  $f_i$  being creation and annihilation operators for spinless fermions, and  $n_i^f = f_i^\dagger f_i$ .

The Green's function for the HCB can be expressed using Eq. (2) as

$$G_{ij} = \langle \Psi_{HCB}^G | b_i b_j^\dagger | \Psi_{HCB}^G \rangle = \langle \Psi_F^G | \prod_{\beta=1}^{i-1} e^{i\pi f_\beta^\dagger f_\beta} f_i^\dagger \prod_{\gamma=1}^{j-1} e^{-i\pi f_\gamma^\dagger f_\gamma} | \Psi_F^G \rangle. \quad (3)$$

$|\Psi_{HCB}^G\rangle$  is the ground state for the HCB and  $|\Psi_F^G\rangle$  is the ground state for the noninteracting fermions. The latter is a Slater determinant, i.e., a product of single particle states  $|\Psi_F^G\rangle = \prod_{\sigma=1}^{N_f} \sum_{\sigma=1}^N P_{\sigma\delta} f_\sigma^\dagger |0\rangle$ , with  $N_f$  the number of fermions ( $N_f = N_b$ ),  $N$  the number of lattice sites and  $\mathbf{P}$  is the matrix of the components of  $|\Psi_F^G\rangle$ . It is easy to see that the action of  $\prod_{\gamma=1}^{j-1} e^{-i\pi f_\gamma^\dagger f_\gamma}$  on the fermionic ground state in Eq. (3) generates only a change of sign on the elements  $P_{\sigma\delta}$  for  $\sigma \leq j-1$ , and the further creation of a particle at site  $j$  implies the addition of one column to  $\mathbf{P}$  with the element  $P_{jN_f+1} = 1$  and all the others equal to zero [the same applies to the action of  $\prod_{\beta=1}^{i-1} e^{i\pi f_\beta^\dagger f_\beta} f_i^\dagger$  on the left of Eq. (3)]. Then the HCB Green's function can be calculated exactly as

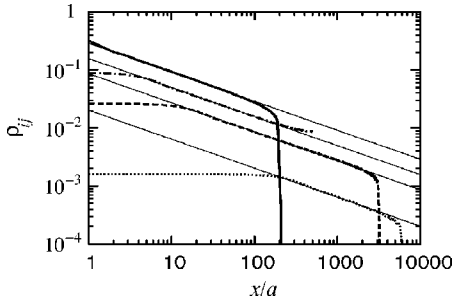


FIG. 1. OPDM vs  $x/a$  ( $x=|x_i-x_j|$ ) for a periodic system with  $\rho=9.1 \times 10^{-2}$ ,  $N_b=91$  (dashed-dotted line), harmonic traps ( $\alpha=2$ ) with  $\bar{\rho}=4.5 \times 10^{-3}$ ,  $N_b=100$  (dashed line) and  $\bar{\rho}=2.7$ ,  $N_b=501$  (thick continuous line, a  $n_i=1$  region is present), and a trap with power  $\alpha=8$ ,  $\bar{\rho}=7.6 \times 10^{-4}$ ,  $N_b=11$  (dotted line). In the trapped cases the abrupt reduction of  $\rho_{ij}$  occurs when  $n_j \rightarrow 0, 1$ , for  $n_i \neq 0, 1$  and  $i$  chosen arbitrarily. Thin continuous lines correspond to power laws  $\sqrt{x/a}$ .

$$G_{ij} = \langle 0 | \prod_{\delta=1}^{N_f+1} \sum_{\beta=1}^N P_{\beta\delta}^{\prime A} \prod_{\sigma=1}^{N_f+1} \sum_{\gamma=1}^N P_{\gamma\sigma}^{\prime B} | 0 \rangle = \det[(\mathbf{P}'^A)^\dagger \mathbf{P}'^B], \quad (4)$$

where  $\mathbf{P}'^A$  and  $\mathbf{P}'^B$  are the new matrices obtained from  $\mathbf{P}$  when the required signs are changed and the new columns added. A proof of the last step in Eq. (4) can be found in Ref. [13]. The evaluation of  $G_{ij}$  is done numerically and the OPDM is given by  $\rho_{ij} = \langle b_i^\dagger b_j \rangle = G_{ij} + \delta_{ij}(1 - 2G_{ii})$ . The NO ( $\phi_i^n$ ) can be determined by the eigenvalue equation  $\sum_{j=1}^N \rho_{ij} \phi_j^n = \lambda_\eta \phi_i^n$ , with  $\lambda_\eta$  being their occupations.

We focus next on the large- $x$  behavior of the OPDM. For the periodic case ( $V_\alpha=0$ ) we obtain that for any density  $\rho \equiv N_b/N \neq 0, 1$  the OPDM decays as a power law  $\rho_{ij} \sim A_\rho / \sqrt{x/a}$  for large  $x$  (Fig. 1), where  $A_\rho$  depends only on the density ( $a$  is the lattice constant). This behavior was found before by means of exact analytical treatments [6]. In the

presence of a confining potential, the case relevant for the experiments with ultracold atoms, the situation is more complicated since the system loses translational invariance and no analytical results are available. We first analyze the case where  $n_i < 1$  all over the system. We find, remarkably, that in this case the OPDM decays as a power law  $\rho_{ij} \sim A_\rho^\alpha |x/a|^{-1/2}$  for large  $x$ , i.e., independently of the local changes of the density. (They become relevant only when  $n_i, n_j \rightarrow 0$ .)  $A_\rho^\alpha$  depends on the characteristic density of the system  $\bar{\rho} = N_b a / \zeta$  and the power  $\alpha$  of the confining potential.  $\zeta = (V_\alpha/t)^{-1/\alpha}$  is a length scale of the trap in the presence of the lattice [14]. Moreover, the exponent of the OPDM power-law decay does not depend on the power  $\alpha$  of the confining potential, i.e., it is universal (Fig. 1).

A drastic difference between the continuous case and the one with a lattice is the possibility to build up regions with densities  $n_i=1$ , so that such sites are not any more coupled coherently to the rest. Once such regions appear, many NO become occupied with  $\lambda_\eta=1$ , and all the other NO (with  $\lambda_\eta \neq 1$ ) become pairwise degenerated since the system is split in two identical part by the  $n_i=1$  plateau [Figs. 2(b) and 2(c)]. Even in this case we find that the OPDM decays as a power law  $\rho_{ij} \sim A_\rho^\alpha |x/a|^{-1/2}$  for large  $x$  in the regions away from  $n_i, n_j \neq 0, 1$  (Fig. 1).

The universal behavior of the OPDM at large- $x$  above shows that although the 1D HCB gas does not exhibit BEC in the TL [15], quasi-long-range order is present and a large occupation of the lowest NO can occur. In the periodic case the NO are plane waves, so that their occupation and the MDF coincide. The results for the large- $x$  behavior of the OPDM in the periodic case imply that in the TL  $n_{k=0}$  scales as  $\sqrt{N_b}$  at constant  $\rho$ , and  $n_k$  diverges as  $|k|^{-1/2}$  for  $k \rightarrow 0$  and  $N_b \rightarrow \infty$ , i.e., in the same way as in the case without a lattice [4,5].

In the trapped system, due to loss of translational invariance, the NO and the MDF do not coincide. To obtain the behavior of the lowest NO in the TL, we study how it scales when the strength of the trap (or the number of particles) is

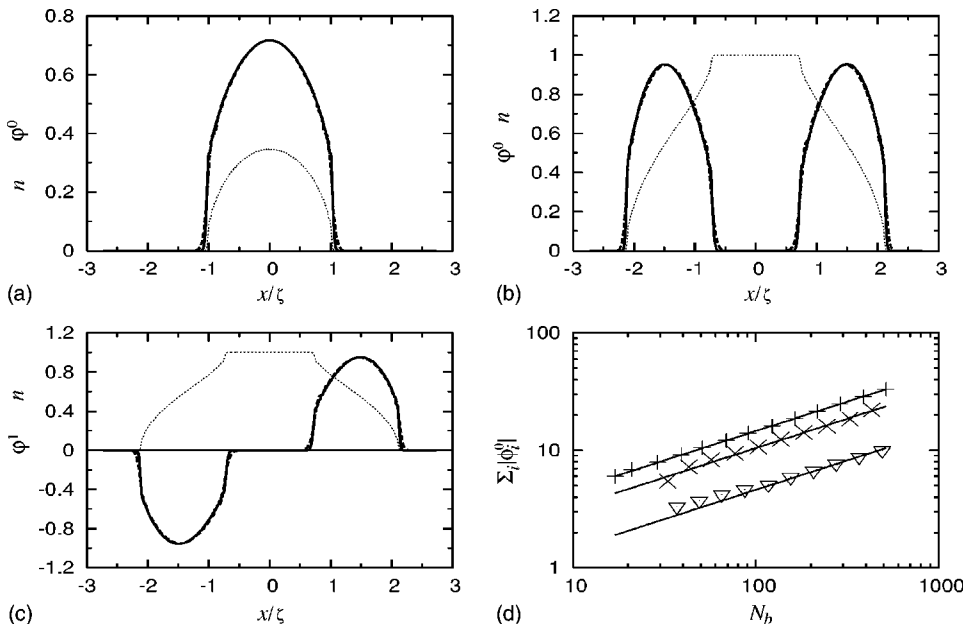


FIG. 2. Scaled lowest NO and density profiles (thin dotted lines) for harmonic traps with (a)  $\bar{\rho}=0.55$ ,  $N_b=101$  (continuous line),  $N_b=30$  (dashed line); (b), (c)  $\bar{\rho}=3.0$ ,  $N_b=551$  (continuous line),  $N_b=167$  (dashed line); (d) shows  $\sum_i |\phi_i^0|$  vs  $N_b$ , in traps with power  $\alpha=8$  of the confining potential, for  $\bar{\rho}=1.0(+), 2.0(\times), 2.25(\nabla)$ , a  $n_i=1$  region is present); continuous lines correspond to power laws  $\sqrt{N_b}$ .

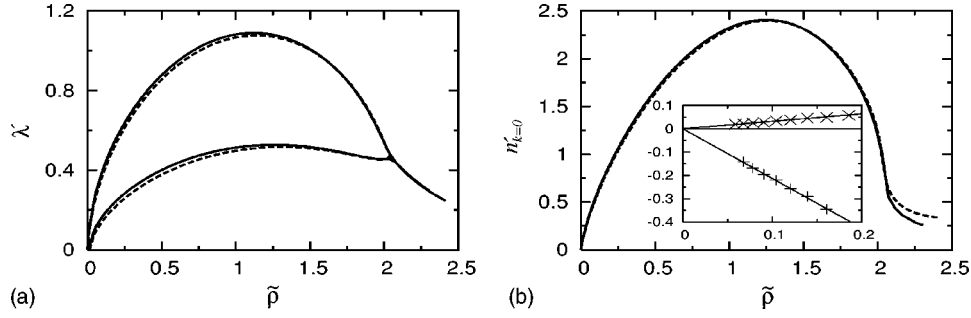


FIG. 3.  $\lambda'$  of the two lowest NO (a) and  $n'_{k=0}$  (b) vs the characteristic density ( $\tilde{\rho}$ ) for traps with power of the confining potential  $\alpha=8$ ,  $V_8 a^8=2.0 \times 10^{-19}t$  (continuous line) and  $V_8 a^8=1.0 \times 10^{-15}t$  (dashed line). The inset in (b) shows  $\delta\lambda'_0$  for  $\tilde{\rho}=1.0$  ( $\times$ ) and  $\delta n'_{k=0}$  for  $\tilde{\rho}=2.25$  ( $+$ ) vs  $(\zeta/a)^{-1/2}$  (see text); the continuous lines show linear behavior.

changed keeping the characteristic density constant. In Figs. 2(a)–2(c) we show the results obtained for the lowest NO in harmonic traps where the curvature of the confining potential was changed by one order of magnitude. It can be seen that a scaled NO  $\varphi^0=R^{1/2}\phi^0$  exists, which does not change when any parameter of the system is changed keeping  $\tilde{\rho}$  constant. Even when regions with  $n_i=1$  are present [Figs. 2(b) and 2(c)] where the two lowest NO are degenerate, the scaled NO exist. Here, the length scale  $\zeta$  set by  $V_\alpha$  determines the length  $L=B_\rho^\alpha\zeta$  over which a nonvanishing density is present.  $B_\rho^\alpha$  depends on the characteristic density  $\tilde{\rho}$  and the power  $\alpha$  of the confining potential.

The scaling factor  $R$  is defined for any confining potential as  $R=\sqrt{N_b}\zeta/a$ . A measure of the scaling of the NO can be obtained by studying the area below them. If the above-mentioned scaling is valid, since this area is expected to depend only on  $\tilde{\rho}$ , we have  $\int dx |\varphi^0(x/\zeta)|/\zeta \sim R^{1/2}(a/\zeta)\sum_i |\phi_i^0| = S_\rho$  implying that  $\sum_i |\phi_i^0| = S'_\rho \sqrt{N_b}$  ( $S_\rho$  and  $S'_\rho$  depend only on  $\tilde{\rho}$ ). Figure 2(d) shows the results obtained for  $\sum_i |\phi_i^0|$  vs  $N_b$  (at constant  $\tilde{\rho}$ ) in traps with power  $\alpha=8$  of the confining potential [16]. It can be seen that already for  $N_b > 100$  the expected power law  $\sqrt{N_b}$  is present, confirming our previous statements for large enough systems.

With the findings above, the leading behavior of the lowest NO  $\lambda_0 = \sum_{ij} \phi_i^0 \rho_{ij} \phi_j^0$  can be evaluated in the TL and for a given  $\tilde{\rho}$  as follows. Replacing the sums in  $\lambda_0$  by integrals ( $L \gg a$ ) one obtains

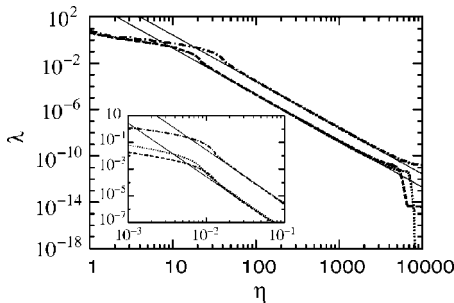


FIG. 4. Occupation of the NO vs  $\eta$  in systems with  $N=10\,000$ :  $N_b=21$  periodic case (dashed-dotted line),  $N_b=11$ ,  $V_2 a^2=5.0 \times 10^{-12}t$  (dashed line), and  $N_b=11$ ,  $V_8 a^8=5.0 \times 10^{-34}t$  (dotted line). The inset shows  $n_k$  vs  $ka$  for the same parameters and the same notation. Thin continuous lines correspond to power laws  $\eta^{-4}$ , and  $k^{-4}$  in the inset.

$$\begin{aligned} \lambda_0 &\sim (1/a^2) \int_{-L}^L dx \int_{-L}^L dy \frac{\phi^0(x) A_\rho^\alpha \phi^0(y)}{|(x-y)/a|^{-1/2}} \\ &= (\zeta/a)^{3/2} R^{-1} \int_{-B_\rho^\alpha}^{B_\rho^\alpha} dX \int_{-B_\rho^\alpha}^{B_\rho^\alpha} dY \frac{\varphi^0(X) A_\rho^\alpha \varphi^0(Y)}{|X-Y|^{-1/2}} = C_\rho^\alpha \sqrt{\zeta/a} \\ &= D_\rho^\alpha \sqrt{N_b}, \end{aligned} \quad (5)$$

where we did the change of variables  $x=X\zeta$ ,  $y=Y\zeta$ , and  $\phi^0 = R^{-1/2}\varphi^0$ . The integral over  $X, Y$  depends only on the characteristic density. Then for a given confining potential with power  $\alpha$ ,  $C_\rho^\alpha$  and  $D_\rho^\alpha$  depend only on  $\tilde{\rho}$ , demonstrating that  $\lambda_0$  scales in the TL as  $\sqrt{N_b}$ . The same analysis can be done with the MDF, where instead of normalizing it by the system size (as usual for homogeneous systems) we normalize it by the length scale set by the potential [ $n_k=(a/\zeta)\sum_{ij} e^{-ik(i-j)}\rho_{ij}$ ]. Considering the large- $x$  form of the OPDM, and repeating the reasoning above, one obtains that  $n_{k=0}$  also scales as  $\sqrt{\zeta}$  or  $\sqrt{N_b}$ , for constant  $\tilde{\rho}$ , in the TL.

So far we have analyzed the scaling of  $\lambda_0$  and  $n_{k=0}/\sqrt{\zeta/a}$  in the TL. We discuss in what follows its relevance for finite size systems. In Fig. 3 we plot  $\lambda'=\lambda/\sqrt{\zeta/a}$  for the first two NO (a) and  $n'_{k=0}=n_{k=0}/\sqrt{\zeta/a}$  (b) as a function of the charac-

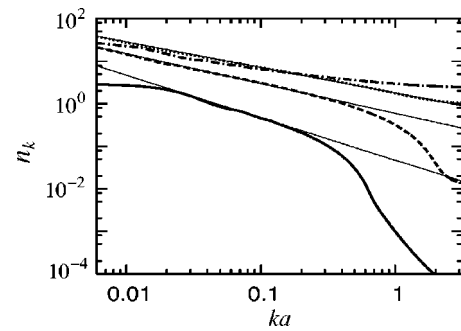


FIG. 5. MDF for systems with  $V_2 a^2=3.0 \times 10^{-5}t$  and  $N_b=11$  (continuous line),  $N_b=101$  (dashed line), and  $N_b=401$  (dotted line),  $N_b=591$  (dashed-dotted line). Accompanying thin continuous lines correspond to power laws:  $k^{-1}$  for  $N_b=11$ ,  $k^{-0.7}$  for  $N_b=101$ , and  $k^{-0.6}$  for  $N_b=401$ .

teristic density for two traps with very different confining potentials with power  $\alpha=8$  [16]. As Fig. 3 shows, finite size corrections to the leading behavior are very small since the values of  $\lambda$  and  $n_{k=0}$  almost scale like in the TL. Actually, the results for the NO are indistinguishable after the region with  $n_i=1$  appears in the system, which is the point where the degeneracy sets in Fig. 3(a). We find the finite size corrections to  $\lambda'$  and  $n'_{k=0}$  to be  $\sim 1/\sqrt{\zeta/a}$  so that  $\lambda_0/\sqrt{\zeta/a}=C_{\tilde{\rho}}-E_{\tilde{\rho}}/\sqrt{\zeta/a}$  and  $n_{k=0}/\sqrt{\zeta/a}=F_{\tilde{\rho}}-G_{\tilde{\rho}}/\sqrt{\zeta/a}$ , where  $C_{\tilde{\rho}}$ ,  $E_{\tilde{\rho}}$ ,  $F_{\tilde{\rho}}$ , and  $G_{\tilde{\rho}}$  depend only on  $\tilde{\rho}$ . In addition  $E_{\tilde{\rho}}$  and  $G_{\tilde{\rho}}$  can be positive or negative depending on the value of  $\tilde{\rho}$ . As an example we plot in the inset of Fig. 3(b)  $\delta\lambda'_0=C_{\tilde{\rho}}-\lambda_0/\sqrt{\zeta/a}$  for  $\tilde{\rho}=1.0$  ( $E_{\tilde{\rho}}$  is positive) and  $\delta n'_{k=0}=F_{\tilde{\rho}}-n_{k=0}/\sqrt{\zeta/a}$  for  $\tilde{\rho}=2.25$  ( $G_{\tilde{\rho}}$  is negative). Similar results were obtained for harmonic traps and the homogeneous system, in the latter case changing  $\zeta/a$  by  $N$ .

Finally, we study the large- $\eta$  behavior of the NO occupations ( $\lambda_\eta$ ). In contrast to the large- $x$  behavior of the density matrix, we do not find a universal feature in the large- $\eta$  behavior of  $\lambda_\eta$  for arbitrary values of the characteristic density  $\tilde{\rho}$ . However, for very small values of  $\tilde{\rho}$  we find that a universal power law develops in the large- $\eta$  region of  $\lambda_\eta$  as is shown in Fig. 4. The power-law decay is in this case of the form  $\lambda_\eta=A_{N_b}/\eta^4$ , where  $A_{N_b}$  depends only on the number of particles in the trap independently of the confining potential, as is shown in Fig. 4. Since this occurs only for very low values of  $\tilde{\rho}$  we expect this behavior to be generic for the continuous limit. This, to our knowledge, has not been discussed before. In the latter limit the high momentum tail of the MDF was found to decay as  $n_k\sim|k|^{-4}$  for HCB in a harmonic trap [17], and for the Lieb-Liniger gas of free and harmonically trapped bosons for all values of the interaction strength [18]. Our results for the MDF (inset in Fig. 4) show that the large- $k$  behavior of  $n_k$  for low  $\tilde{\rho}$  is also universal, irrespective of the confining potential.

At this point it is important to remark that the universal behavior and scaling relations shown in Figs. 1–4 appear

already at moderate number of particles, and hence, are relevant for experiments. However, the  $|k|^{1/2}$  singularity in  $n_k$ , well known from the homogeneous system, is difficult to see explicitly in such situations, in contrast to previous claims [19]. Fitting power laws  $n_k\sim k^{-\beta}$  for finite systems could lead to wrong conclusions about the large- $x$  behavior of the OPDM, as shown in Fig. 5. For very low fillings ( $N_b=11$ ), a “power-law” behavior with  $\beta=1$  may be seen before the  $\beta=4$  is established for large  $k$ . Increasing the number of particles leads to a decrease of  $\beta$ , up to  $\beta=0.6$  ( $N_b=401$ ). Hence, the power  $\beta$  depends strongly on the number of particles and cannot be understood as reflecting any universal property of the system. Power-law behavior disappears only when  $n_i$  reaches 1 in parts of the system ( $N_b=591$  in Fig. 5).

In summary, we have shown that quasi-long-range order is present in 1D HCB on the presence of a lattice, with a universal power-law decay of the OPDM, independent of the power of the confining potential. Furthermore, we have shown how the occupation of the lowest NO and the value of the MDF at zero momentum are determined by the large distance behavior of the OPDM. Even in the cases where a region with  $n_i=1$  builds up in the middle of the system we find that both quantities scale proportionally to  $\sqrt{N_b}$  (at constant  $\tilde{\rho}$ ). A further universal power-law decay has been found for the eigenvalues of the OPDM ( $\lambda_\eta$ ) for large values of  $\eta$  at low densities ( $\lambda_\eta\sim\eta^{-4}$ ). It translates into a corresponding power-law decay of the MDF ( $n_k\sim|k|^{-4}$ ) at large momenta also independently of the power of the confining potential, pointing to scale invariance in the ultraviolet limit of the continuous case.

*Note added.* A HCB gas has been realized very recently on 1D lattices by Paredes *et al.* [20].

We are grateful to HLR-Stuttgart (Project DynMet) for allocation of computer time, and SFB 382 for financial support. We are indebted to F. Göhmann for bringing to our attention Ref. [6].

- 
- [1] M. Olshanii, Phys. Rev. Lett. **81**, 938 (1998); D. S. Petrov, G. V. Shlyapnikov, and J. T. M. Walraven, *ibid.* **85**, 3745 (2000); V. Dunjko, V. Lorent, and M. Olshanii, *ibid.* **86**, 5413 (2001).  
 [2] F. Schreck *et al.*, Phys. Rev. Lett. **87**, 080403 (2001); A. Görlitz *et al.*, *ibid.* **87**, 130402 (2001); M. Greiner *et al.*, *ibid.* **87**, 160405 (2001); T. Stöferle *et al.*, *ibid.* **92**, 130403 (2004).  
 [3] M. Girardeau, J. Math. Phys. **1**, 516 (1960).  
 [4] A. Lenard, J. Math. Phys. **5**, 930 (1964).  
 [5] H. G. Vaidya and C. A. Tracy, Phys. Rev. Lett. **42**, 3 (1979).  
 [6] N. Kitanine, J. M. Maillet, N. A. Slanov, and V. Terras, Nucl. Phys. B **642**, 433 (2002), and references therein.  
 [7] M. A. Cazalilla, J. Phys. B **37**, S1 (2004), and references therein.  
 [8] M. D. Girardeau, E. M. Wright, and J. M. Triscari, Phys. Rev. A **63**, 033601 (2001); T. Papenbrock, *ibid.* **67**, 041601(R) (2003); P. J. Forrester, N. E. Frankel, T. M. Garoni, and N. S. Witte, *ibid.* **67**, 043607 (2003).  
 [9] O. Penrose and L. Onsager, Phys. Rev. **104**, 576 (1956).  
 [10] E. H. Lieb and R. Seiringer, Phys. Rev. Lett. **88**, 170409 (2002).  
 [11] M. Greiner *et al.*, Nature (London) **415**, 39 (2002).  
 [12] P. Jordan and E. Wigner, Z. Phys. **47**, 631 (1928).  
 [13] A. Muramatsu, in *Quantum Monte Carlo Methods in Physics and Chemistry*, edited by M. P. Nightingale and C. J. Umrigar (Kluwer Academic, Dordrecht, 1999).  
 [14] M. Rigol and A. Muramatsu, e-print cond-mat/0311444.  
 [15] C. N. Yang, Rev. Mod. Phys. **34**, 694 (1962).  
 [16] This value of  $\alpha$  was chosen just to show that our analysis is valid for any  $\alpha$  and not only for a harmonic potential.  
 [17] A. Minguzzi, P. Vignolo, and M. P. Tosi, Phys. Lett. A **294**, 222 (2002).  
 [18] M. Olshanii and V. Dunjko, Phys. Rev. Lett. **91**, 090401 (2003).  
 [19] G. E. Astrakharchik and S. Giorgini, Phys. Rev. A **68**, 031602(R) (2003).  
 [20] B. Paredes *et al.*, Nature (London) **429**, 277 (2004).